



## Journal of Renewable Energies

Revue des Energies Renouvelables

journal home page : <https://revue.cder.dz/index.php/rer>

# Performances of Vector Control of Brushless Doubly-Fed Induction Generator Incorporate in Wind Energy Conversion System with TSR MPPT

Razik Dib \*, Abed Khoudir, Katia Kouzi

Electrical Engineering Department University Frères Mentouri Constantine, Algeria

\* Corresponding author, E-mail address: [dibrazik003@gmail.com](mailto:dibrazik003@gmail.com)

Tel.: +213 657775073

### Abstract

Currently, variable speed wind systems based on the Brushless Doubly-Fed Induction Machine (BDFIM) are the most used in Wind Energy Conversion System (WECS). The main features of BDFIM are high reliability due to its brushless operating, lower capital and operational costs. This work presents a field-oriented control scheme for a BDFIG acting as a variable-speed generator. The presented vector control is determined on the power-winding stator-flux frame and can be employed to control both the speed and the reactive power. In addition, use of wind speed sensors by an anemometer, and maximize wind energy extraction Tip Speed Ratio (TSR) Maximum Power Point Tracker (MPPT) is proposed. Several simulation results under different operating conditions are provided to prove the effectiveness of the presented scheme. The obtained results show the efficiency and validity of the proposed control strategy.

**Keywords:** Brushless Doubly-Fed Induction Machine (BDFIM), Wind Energy Conversion System (WECS), Tip Speed Ratio (TSR), Maximum Power Point Tracker (MPPT).

### 1. Introduction

Generation of power from renewable energy sources is more promising due to its clean character and free availability. In the last two decades, research is been carried out specifically on wind power generation systems to capture more power at fluctuating wind speeds. With rapid development of wind turbine and power electronic technology. The Wind power generation systems with brushless doubly-fed generator (BDFIG) are of the following characteristics: 1) vector control is applied to realize the decoupling control of active power and reactive power so that it is able to not only achieve maximum power point tracking (MPPT),

but support grid voltage as well,2) its reliability is expected to be improved and it is more suitable to be used even in severe weather conditions because the brush and slip rings are eliminated in BDFIG,3) the feeding converter only has to handle a partially rated power of BDFIG (the slip power), which means significant cost savings, compared with conventional systems with fully rated converter. Consequently, the wind power system with BDFIG is becoming one of the development trends worldwide in wind power generation field [1]. A no-load mode simulation of cascade brushless doubly fed generator (BDFIG) was built according to the d-q mathematical model based on the double synchronous reference frame [2]. This paper presented BDFIG analysis in detail and relying on the vector control algorithm via regulating the power as independent control of the active and reactive power of PW. The maximum power point tracking (MPPT) was implemented for optimal energy capture by the wind turbine MPPT with Tip Speed Ratio was confirmed by a simulation study and the system performance were evaluated in detail.

## 2. Model mathematic

### 2.1 Modeling of the wind energy conversion system

#### 2.1.1 Modelling of the wind turbine and gearbox

Before the description of the wind turbine first let's see its principle of function. The blades of the turbine are making in move by the kinetic energy of wind having the transformation of these energy to mechanical power and that make the turbine shift in rotation which train the generator, so the first thing to build the mathematical model is defining the wind power[12]:

$$P_w = \frac{1}{2} \rho S v^3 \quad (1)$$

During the wind movement across the wind turbine the wind loses some speed by the flexible collisions with the blades. But behind the tower the wind keeps moving and that mean the wind turbine can't take all the available kinetic energy of wind but there is a limit knowing as the Betz limit or the power coefficient  $C_p=16/27$ . Many researches were done to define the approximate formula of this coefficient but in this paper, we choose the next expression[12]:

$$\left\{ \begin{array}{l} C_p = 0.5176 \left( \frac{116}{\lambda_i} - 0.4\beta - 5 \right) e^{\frac{21}{\lambda_i}} \\ \frac{1}{\lambda_i} = \frac{1}{\lambda + 0.08\beta} - \frac{0.035}{\beta^3 + 1} \\ \lambda = \frac{R\omega_m}{v} \\ \omega_m = \frac{\Omega}{G} \end{array} \right. \quad (2)$$

$$P_T = \frac{1}{2} C_p \rho S v^3 \quad (3)$$

$$T_m = \frac{C_p \rho S v^3}{2 \omega_m} \quad (4)$$

### 2.1.2 Dynamical model of the BDFIG

The BDFIG has two three-phase stator windings but with a different number of the pole pairs. One of the windings is supplied with the grid voltage with the frequency  $f_s$  and has  $p_p$  pole pairs namely power winding (PW), the other is supplied with the voltage having controlled the amplitude and the frequency  $f_c$  and has  $p_c$  pole pairs namely control winding (CW). Since the windings have different pole numbers, they do not link directly, but they are coupled through the rotor that has  $n = p_p + p_c$  pole numbers (not pairs). In order to produce the co-operative torque with both windings in the rotor, the conditions  $p_p \omega_r = \omega_p$  and  $p_c \omega_r = \omega_c$  have to be kept, from which [6].

$$\omega_r = \frac{\omega_p - \omega_c}{P_p + P_c} \quad (5)$$

The electrical equations of the BDFIG in the synchronous reference frame (d-q) are this given by [5][11].

$$\begin{cases} V_{dp} = R_p \cdot I_{dp} + \frac{d\Psi_{dp}}{dt} - \omega_p \cdot \Psi_{qp} \\ V_{qp} = R_p \cdot I_{qp} + \frac{d\Psi_{qp}}{dt} + \omega_p \cdot \Psi_{dp} \end{cases} \quad (6)$$

$$\begin{cases} V_{dc} = R_c \cdot I_{dc} + \frac{d\Psi_{dc}}{dt} - \omega_c \cdot \Psi_{qc} \\ V_{qc} = c \cdot I_{qc} + \frac{d\Psi_{qc}}{dt} + \omega_c \cdot \Psi_{dc} \end{cases} \quad (7)$$

$$\begin{cases} 0 = R_r \cdot I_{dr} + \frac{d\Psi_{dr}}{dt} - \omega_r \cdot \Psi_{qr} \\ 0 = R_r \cdot I_{qr} + \frac{d\Psi_{qr}}{dt} + \omega_r \cdot \Psi_{dr} \end{cases} \quad (8)$$

$$\omega_r = \omega_p - P_p \cdot \omega, \quad \omega_c = \omega_p - (P_p + P_c) \quad (9)$$

The expressions for stator and rotor flux linkages are, [6][5]

$$\begin{cases} \Psi_{dp} = L_p \cdot I_{dp} + M_p \cdot i_{dr} \\ \Psi_{qp} = L_p \cdot I_{qp} + M_p \cdot i_{qr} \end{cases} \quad (10)$$

$$\begin{cases} \Psi_{dc} = L_p \cdot I_{dc} + M_c \cdot i_{dr} \\ \Psi_{qc} = L_p \cdot I_{qc} + M_c \cdot i_{qr} \end{cases} \quad (11)$$

$$\begin{cases} \Psi_{dr} = L_r \cdot I_{dr} + M_p \cdot i_{dp} + M_c \cdot i_{dc} \\ \Psi_{qr} = L_r \cdot I_{qr} + M_p \cdot i_{qp} + M_c \cdot i_{qc} \end{cases} \quad (12)$$

The Electromagnetic torque is calculated as [7]:

$$T_{em} = \frac{3}{2} P_p (\Psi_{dp} \cdot i_{qp} - \Psi_{qp} \cdot i_{dp}) + \frac{3}{2} P_c (\Psi_{dc} \cdot i_{qc} - \Psi_{qc} \cdot i_{dc}) \quad (13)$$

The active and reactive powers of the PW are defined as [11]:

$$\begin{cases} P_p = \frac{3}{2}(V_{dp}.idp + V_{qp}.iqp) \\ Q_p = \frac{3}{2}(V_{qp}.idp - V_{dp}.iqp) \end{cases} \quad (14)$$

The three-phase voltages  $V_p$  and  $V_c$  are converted in the voltages  $V_{dp}$ ,  $V_{qp}$ ,  $V_{dc}$ , and  $V_{qc}$  with the help of the Park transformation with angles  $\theta_p = \int \omega_p dt$ , and  $\theta_c = \theta_p - (P_p + p_c) \theta_r$ , where  $\theta_r$  is the rotor angle the integral of its rotation speed.

## 2.2 Vector control of the BDFM

In order to be able easily control the electricity production of the wind turbine, the principle of vector control lies in the orientation of the flux in the machine to the stator, to the rotor, or to the air gap according to one of the two axes d or q. The main goal of vector control is the decoupled control of the rotor flux and electromagnetic torque of the generator to obtain high dynamic and static performance [7],(Fig. 1). This scheme is based on the cascade regulation method. Two independent regulation paths are implemented:

Reactive power control:

$$Q_p \rightarrow idp^* \rightarrow idc^* \rightarrow V_{dc}^*$$

Active power electromagnetic torque or speed Control:

$$P_p \rightarrow iqp^* \rightarrow iq c^* \rightarrow V_{qc}^*.$$

Or

$$T_{em} \rightarrow iqp^* \rightarrow iq c^* \rightarrow V_{qc}^*.$$

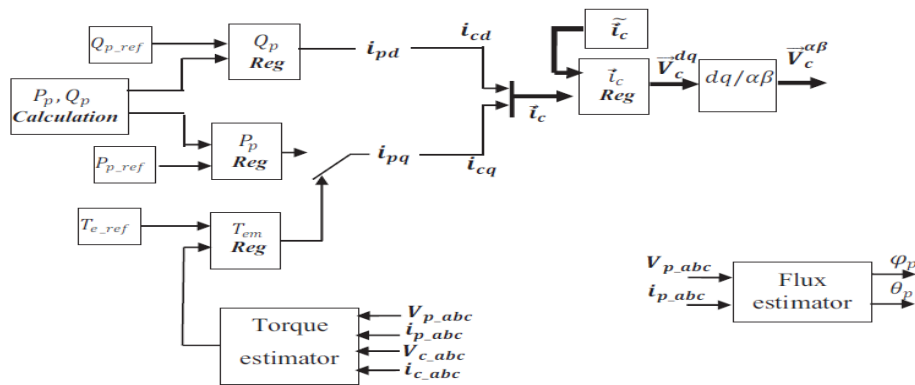


Fig 1. Vector control scheme of BDFIM using a PI regulator

### 2.2.1 Control of the BDFG with a PW field oriented

The best-suited reference frame for the proposed control principle is the PW flux orientation, so,  $\Psi_{dp} = \Psi_p$  and  $\Psi_{qp} = 0$ . If the d-axis of the PW synchronous reference frame is aligned

with the PW air gap flux, the  $R_p$  is neglected. Then, the relation between the PW voltage and  $\Psi_p$  is [2].

$$\begin{cases} V_{dp} = 0, \\ V_{qp} = V_p = \omega_p \cdot \Psi_p, \end{cases} \quad (15)$$

$$\begin{cases} \Psi_{dp} = L_p \cdot i_{dp} + M_p \cdot i_{dr}, \\ 0 = L_p \cdot i_{qp} + M_p \cdot i_{qr}, \end{cases} \quad (16)$$

### 2.2.2 Control of PW current

To find of the ratio between the currents of the PW and the CW we consider the flux of the PW as a variable fixed by the supply voltage (independent variable). the relation between  $i_p$  and  $i_c$  gives as[7]:

$$\frac{d i_{dc}}{dt} = a_{xdc} (i_{dp}) + a_{ydc} (i_{qc}, i_{qp}, \Psi_p). \quad (17)$$

$$\frac{d i_{qc}}{dt} = a_{xqc} (i_{qp}) + a_{yqc} (i_{dc}, i_{dp}, \Psi_p). \quad (18)$$

Where  $a_{xdc}$ ,  $a_{xqc}$  direct relation between  $i_p$  and  $i_c$ . If in the control diagram we add the terms  $a_{ydc}$  and  $a_{yqc}$  through direct action (feed forward)[7].

$$a_{xdc} = \frac{R_r \cdot L_p}{M_c \cdot M_p} i_{dp} + \sigma_p \frac{L_p \cdot L_r}{M_p \cdot M_c} \frac{d i_{dp}}{dt}. \quad (19)$$

$$a_{xqc} = \frac{R_r \cdot L_p}{M_c \cdot M_p} i_{qp} + \sigma_p \frac{L_p \cdot L_r}{M_p \cdot M_c} \frac{d i_{qp}}{dt}. \quad (20)$$

$$a_{ydc} = -\frac{R_r}{M_c \cdot M_p} \Psi_p - \omega_p \frac{\sigma_p \cdot L_p \cdot L_r}{M_p \cdot M_c} i_{qp} + \omega_p \cdot i_{qc}. \quad (21)$$

$$a_{yqc} = \omega_p \frac{\sigma_p \cdot L_p \cdot L_r}{M_p \cdot M_c} i_{dp} - \omega_p \cdot i_{dc} - \omega_p \frac{L_r}{M_c \cdot M_p} \Psi_p. \quad (22)$$

$$\text{Where } \sigma_p = 1 - \frac{M_p^2}{L_p \cdot L_r} \quad (23)$$

$$i_p(s) = \frac{K_p}{\tau_p s + 1} a_{xc}(s), \quad K_p = \frac{M_p \cdot M_c}{L_p \cdot R_r}, \quad \tau_p = \frac{\sigma_p \cdot L_r}{R_r} \quad (24)$$

The linear regulator gives the value  $a_{xc}$ , and by integrating  $a_c$  we obtain the set value of  $i_c$ . Where  $a_c = a_{xc} + a_{yc}$

### 2.2.3 Control of CW current

We obtained the voltage equation  $V_c$  in terms of  $i_c$ . from the the electrical equations of the BDFIG

$$V_{dc} = V_{xdc} (i_{dc}) + V_{ydc} (i_{qc}, i_{dp}, i_{qp}, \Psi_p). \quad (25)$$

$$V_{qc} = V_{xqc}(i_{qc}) + V_{yqc}(i_{dc}, i_{dp}, i_{qp}, \Psi_p) \quad (26)$$

The first term shows direct relation between  $V_c$  and  $i_c$ , the second term presents a cross coupling with lower order compared to the first terms, and therefore can be neglected. The transfer function has first order [7].

$$i_c(s) = \frac{K_c}{\tau_p s + 1} v_c(s) \quad K_c = \frac{1}{R_c}, \tau_c = \frac{L_c - \frac{M_c^2}{L_r \sigma_p}}{R_c}. \quad (27)$$

#### 2.2.4 Control of torque

$$T_{em} = \frac{3}{2}(P_p + P_c) \cdot \Psi_p i_{qp} \quad (28)$$

This term shows the fact that the torque of the BDFM is directly related to  $i_{qp}$ .

#### 2.2.5 PW power control

The active and reactive powers of the PW exchanged with the machine depend only on the PW stator electric variable as has equation (14). The PW is connected to the 50 Hz grid constant voltage, so the PW flux is maintained almost constant. In this way  $Q_p$ , can be directly controlled by an adequate choice of  $i_{dp}$ . Since the active power can be directly controlled using the  $i_{qp}$  reference value [7][11].

$$\begin{cases} Q_p = \frac{3}{2} \omega_p \cdot \Psi_p i_{dp} \\ P_p = \frac{3}{2} \omega_p \cdot \Psi_p i_{qp} \end{cases} \quad (29)$$

### 2.3 Maximum power point tracking (MPPT) control

The main goal of using a MPPT algorithm is to operate the WECS around the maximum power for any variations of the wind speed. Several control schemes have been developed to perform the maximum power point tracking (MPPT) such as MPPT with Turbine Power Profile, MPPT with Optimal Torque Control, MPPT with Optimal Tip Speed Ratio [9]. In this paper we are interested on the TSR MPPT.

#### 2.3.1 MPPT with tip speed ratio

The TSR control method regulates the rotational speed of the generator in order to maintain the TSR to an optimum value at which power extracted is maximum. This method requires both the wind speed and the turbine speed to be measured or estimated in addition to requiring the knowledge of optimum TSR of the turbine in order for the system to be able extract maximum possible power. (Fig. 2) shows the block diagram of a WECS with TSR control.

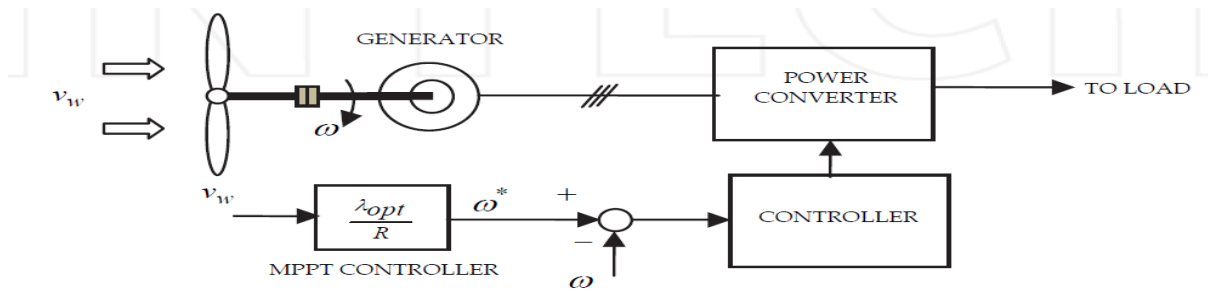


Fig 2. MPPT with Tip Speed Ratio of wind turbines.

### 3. Results and discussion

In order to show the performance given by the proposed scheme control of WECS based on BDFIG with TSR MPPT, various numerical simulation were done for a 2.5KW BDFIG.

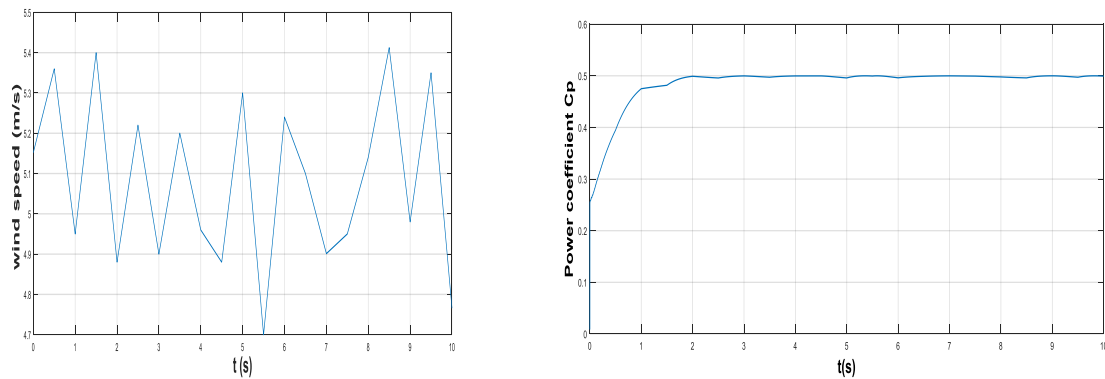


Fig 3. Power coefficient of rotor blades and wind speed

This result shows that, when the wind profile changes,  $C_p$  can quickly reach around the optimal value. The power coefficient is kept around its optimum when  $C_{p-max} = 0.5$

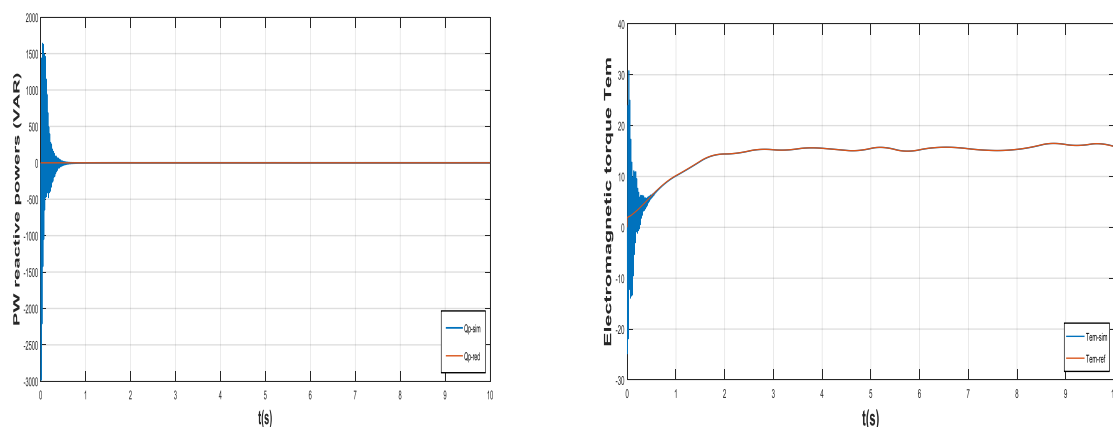


Fig 4. The electromagnetic torque and reactive powers

The electromagnetic torque and its reference we get from MPPT with STR, which represents a good track of its reference and the reactive power which is kept zero. and verifies the decoupling between the electromagnetic torque and reactive power

From(Fig.5) and (Fig.6) it can be seen that correspond to the currents  $i_{dp}$ ,  $i_{qp}$  of the PW and  $i_{dc}$ ,  $i_{qc}$  of the CW. These currents can increase or decrease depending on the wind conditions.

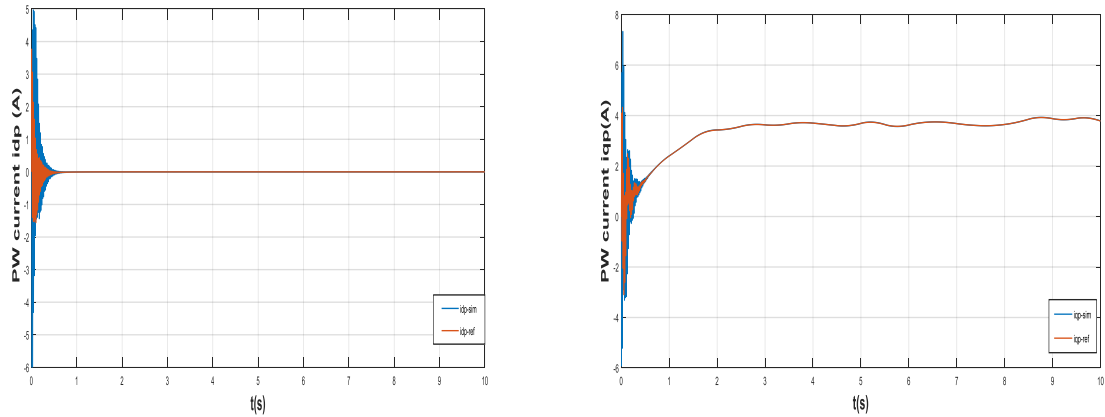


Fig 5. d-q PW current

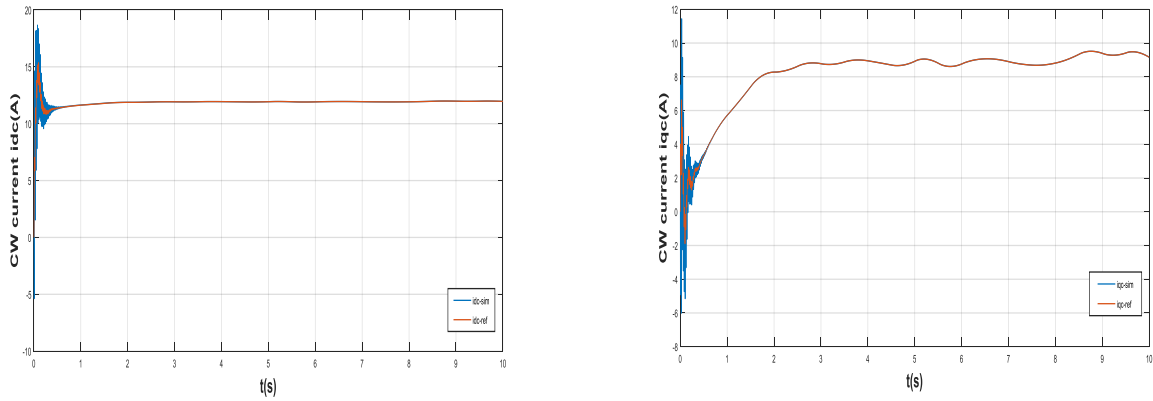


Fig 6. d-q CW current

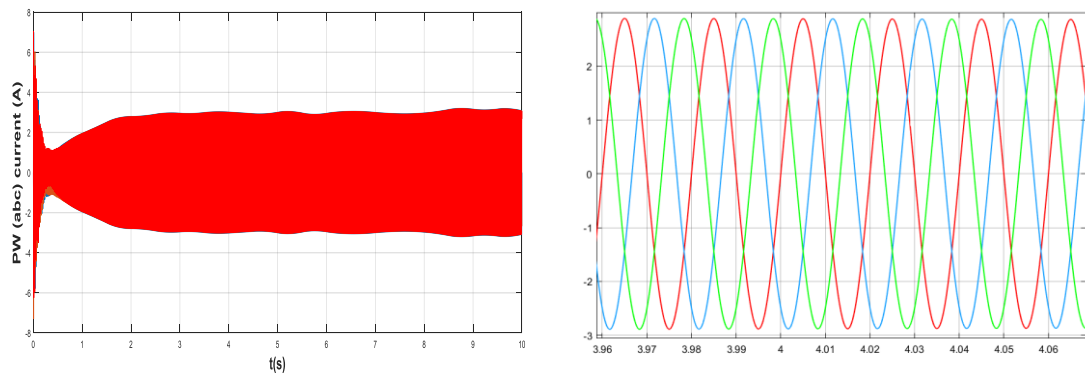


Fig 7. PW (abc) current

Fig.7 represents the temporal evolution of the stator phase currents  $i_{abc}$  of PW. We note that these currents have a constant frequency whatever the operating regime .

Fig.8 shows the temporal evolution of the phase currents  $i_{abc}$  of CW. We notice that these currents have a variable frequency which changes with the speed of rotation.

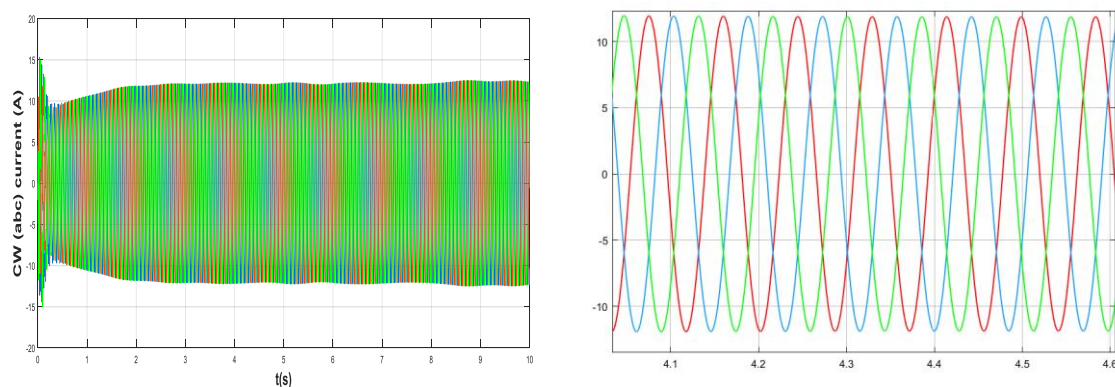


Fig 8. CW (abc) current

Consequently, between the active and reactive powers, this leads to a good control of the power flow between grid and the machine at all time and the MPPT with TSR can be realized. In the end, it can be observed from the simulation result that the control of system BDFG-wind turbine has good performance

#### 4. Conclusions

In this paper, a vector control of brushless doubly-fed induction machine associated in WECS which is driving by TSR MPPT was well explained. To guarantee the maximum generator power with weak oscillations and fast enough to keep up the wind speed variation with the optimal  $\lambda$  and the maximal  $C_p$  an TSR MPPT has proposed.

The obtained simulation results prove the validity of the proposed scheme control and the advantage of working with TSR MPPT to make the wind turbine operate at its optimum power point for large range of wind speed even in the presence of very variable wind speed.

#### 5. References

- [1] Liu, G., Wang, S., & Zhang, R. Modeling and Control of BDFG-based Wind Power Generation Systems under Grid Voltage Sag. In 2009 Asia-Pacific Power and Energy Engineering Conference (pp. 1-5). IEEE. (2009, March).
- [2] Serhoud, H., & Benattous, D. Simulation of grid connection and maximum power point tracking control of brushless doubly-fed generator in wind power system. *Frontiers in Energy*, 7(3), 380-387. (2013).
- [3] Eltamaly, A. M., & Farh, H. M. Maximum power extraction from wind energy system based on fuzzy logic control. *Electric Power Systems Research*, 97, 144-150. (2013).
- [4] YARAMASU, Venkata et WU, Bin. *Basics of Wind Energy Conversion Systems (WECS)*, Model predictive control of wind energy conversion systems. John Wiley & Sons,

2016.

- [5] Tir, Z., & Abdessemed, R. Control of a wind energy conversion system based on brushless doubly fed induction generator. *Revue des Energies Renouvelables*, 17(1), 55-69. (2014).
- [6] Viktor.P,2017, *Electric Generators, Renewable Energy Systems: Simulation with Simulink® and SimPowerSystems™*. Crc Press, 2016.
- [7] Lobo, F. J. P. *COMMANDE DE LA BDFM. Modélisation, conception et commande d'une machine asynchrone sans balais doublement alimentée pour la génération à vitesse variable (Doctoral dissertation)*. (2003).
- [8] JOHN W & SONS,I, *Fundamentals of Wind Energy Conversion System Control, POWER CONVERSION AND CONTROL OF WIND ENERGY SYSTEMS*, R. Abhari J. Anderson F. Cañavero , Canada,(pp32-36). 2011.
- [9] Asri, A, "Intelligent maximum power tracking control of a PMSG wind energy conversion system." *Asian Journal of Control* 21.4 (2019)
- [10] Kumar, D., & Chatterjee, K. A review of conventional and advanced MPPT algorithms for wind energy systems. *Renewable and sustainable energy reviews*, 55, 957-970. (2016).
- [11] Rahab, A., Senani, F., & Benalla, H. Direct power control of brushless doubly-fed induction generator used in wind energy conversion system. *International Journal of Power Electronics and Drive System (IJPEDS)*, 8(1), 417-433. (2017).
- [12] Trejos-Grisales, L., Guarnizo-Lemus, C., & Serna, S. Overall description of wind power systems. *Ingeniería y Ciencia*, 10(19), 99-126. (2014).